INTERNATIONAL JOURNAL FOR NUMERICAL METHODS IN FLUIDS
Int. J. Numer. Meth. Fluids 2007; **54**:1327–1350
Published online 7 February 2007 in Wiley InterScience (www.interscience.wiley.com). DOI: 10.1002/fld.1429

Two-dimensional adaptive mesh generation

Yaoxin Zhang*,†,‡, Yafei Jia§ and Sam S. Y. Wang¶

National Center for Computational Hydroscience and Engineering, The University of Mississippi, 102 Carrier Hall, MS 38677, U.S.A.

SUMMARY

In this paper, a two-dimensional adaptive elliptic mesh generation system, derived from the Ryskin and Leal (RL) orthogonal mesh generation system based on the orthogonal condition (orthogonality) and the cell area equal-distribution principle (adaptivity), is presented. The proposed generation system takes into account not only the mesh orthogonality and adaptivity but also the mesh smoothness by adopting a method that the distortion functions is determined by both the scale factors and the averaged scale factors of the constant mesh lines. Examples and application show that the proposed generation system is effective and easy to use. Copyright © 2007 John Wiley & Sons, Ltd.

Received 10 August 2006; Accepted 2 December 2006

KEY WORDS: adaptive mesh generation; equal distribution; adaptivity; orthogonality; smoothness

1. INTRODUCTION

Accurate and efficient analysis of computational fluid dynamics (CFD) demands high-quality computational mesh. In general, mesh quality is evaluated by two standard academic criterions: orthogonality and smoothness. For a particular CFD problem, however, even if a computational mesh satisfies the above two criterions, a good solution may not be obtained if this mesh does not consider the mesh density distribution (adaptivity). For example, in flow field the region with large gradient variations, usually not a *priori*, desires more mesh lines. Mesh generation ought, therefore, to consider not only the geometry, but also the physics of the solutions adaptively.

*Correspondence to: Yaoxin Zhang, National Center for Computational Hydroscience and Engineering, The University of Mississippi, 102 Carrier Hall, MS 38677, U.S.A.
†E-mail: yzhang@ncche.olemiss.edu
‡Research Scientist.
§Research Professor and Assistant Director for Basic Research.
¶F.A.P Barnard Distinguished Professor and Director.

Contract/grant sponsor: USDA Agriculture Research Service; contract/grant number: 58-6408-2-0062

In the last 20 years, many techniques and methodologies [1–10] on adaptive mesh generation have been developed. Basically, these techniques can be grouped into three categories: h-methods (local refinement or coarsening) [11]; m-methods (remeshing or regeneration); and r-methods (redistribution or repositioning) [1–10]. The h-methods are straightforward and easy to understand, but the bookkeeping and the data structures are very complicated, while the m-methods can produce high-quality meshes but at a cost of heavy computational effort. As for the r-methods, the adaptive mapping is usually fulfilled through some suitable generation equations. The main concern of this paper is the r-method.

The r-methods are usually associated with the so-called equal-distribution principle, which was first proposed and applied in one dimension. In the equal-distribution principle, a certain property of the mesh is equidistributed based on some weighting function (or monitor function) which represents the characteristic of the solutions. In CFD applications, it is found that the global error can be reduced when the error is equidistributed, i.e. the error is the same for all the cells of the mesh (called isotropic adaptation).

According to Cao *et al*. [4], the r-methods can be further divided into two groups: the location-based methods [1–3, 5, 6, 8–10], which directly control the position of the mesh nodes, and the velocity-based methods [4] and [7], which control the mesh velocity. The deformation method proposed by Liao and Anderson [7] and the method of geometric conservation law (GLC) developed by Cao *et al*. [4] are two typical representatives of the second group. In the first group, Winslow [10] first developed an adaptive elliptic generation system by introducing a diffusion coefficient which is related to solution gradients into a Laplace equation. Thompson *et al*. [9] proposed a Poisson equation system with control functions (often referred as TTM system). Although it is capable of adjusting grid spacing and direction, the TTM system is originally not for adaptive mesh generation. Based on this Poisson equation system, Anderson [1] proposed a set of control functions to control the arc length adaptively; and, Lee [6] derived, without approximations, a set of control functions satisfying the area equal-distribution concept. Brackbill and Saltzman [3] developed a variational adaptive generation system by minimizing the functional which combines the mesh orthogonality, smoothness, and adaptivity (density distribution). However, the complexity of this system makes it difficult to use. Knupp [5] also used the variational approach to derive an adaptive elliptic generation system. Sun [8] used the area-preserving map and the classical conformal map to control the cell area equal distribution and cell shape.

In this paper, a new mesh redistribution method (r-method) is developed. The elliptic adaptive generation system is derived from the famous orthogonal mapping system proposed by Ryskin and Leal [12] (often referred as RL system) according to the orthogonal condition (orthogonality) and the cell area equal-distribution principle (adaptivity). By adopting a smoothing technique proposed by Zhang *et al*. [13] that the distortion function is determined by both the scale factors and the averaged scale factors of the constant mesh lines into the system, the proposed adaptive generation system is capable of producing meshes considering not only mesh orthogonality and adaptivity but also smoothness. Several examples and an application to a natural river will be used to demonstrate the proposed adaptive generation system.

2. ELLIPTIC ADAPTIVE MESH GENERATION SYSTEMS

2.1. RL system

In 1983, Ryskin and Leal [12] proposed a well-known orthogonal mapping system. In this system, the orthogonal mapping between the physical coordinates $(x^i(\equiv x, y), i = 1, 2)$ and the

DOI: 10.1002/fld

computational coordinates ($\xi^i (\equiv \xi, \eta)$, $i = 1, 2$) is described using the following covariant Laplace equations:

$$\frac{\partial}{\partial \xi}\left(f \frac{\partial x}{\partial \xi} \right) + \frac{\partial}{\partial \eta}\left(\frac{1}{f} \frac{\partial x}{\partial \eta} \right) = 0 \tag{1a}$$

$$\frac{\partial}{\partial \xi}\left(f \frac{\partial y}{\partial \xi} \right) + \frac{\partial}{\partial \eta}\left(\frac{1}{f} \frac{\partial y}{\partial \eta} \right) = 0 \tag{1b}$$

In Equation (1), the distortion function f (also called aspect ratio) is defined as the ratio of the scale factors in ξ and η directions (h_ξ and h_η):

$$f = \frac{h_\eta}{h_\xi} = \left(\frac{x_\eta^2 + y_\eta^2}{x_\xi^2 + y_\xi^2} \right)^{1/2} \tag{2a}$$

$$h_\xi = g_{11}^{1/2}, \quad h_\eta = g_{22}^{1/2} \tag{2b}$$

where the metric tensor g_{ij} is defined as follows:

$$g = \begin{vmatrix} (x_\xi^2 + y_\xi^2) & (x_\xi x_\eta + y_\xi y_\eta) \\ (x_\xi x_\eta + y_\xi y_\eta) & (x_\eta^2 + y_\eta^2) \end{vmatrix} \tag{3}$$

and $x_\xi = \partial x / \partial \xi$ and so forth.

Using the central difference scheme, Equation (1) can be discretized as follows:

$$F_{i,j} x_{i,j} = f_{i+1/2,j} x_{i+1,j} + f_{i-1/2,j} x_{i-1,j} + \frac{1}{f_{i,j+1/2}} x_{i,j+1} + \frac{1}{f_{i,j-1/2}} x_{i,j-1} \tag{4a}$$

$$F_{i,j} y_{i,j} = f_{i+1/2,j} y_{i+1,j} + f_{i-1/2,j} y_{i-1,j} + \frac{1}{f_{i,j+1/2}} y_{i,j+1} + \frac{1}{f_{i,j-1/2}} y_{i,j-1} \tag{4b}$$

where

$$F_{i,j} = f_{i+1/2,j} + f_{i-1/2,j} + \frac{1}{f_{i,j+1/2}} + \frac{1}{f_{i,j-1/2}}$$

The RL system is attractive due to its effectiveness on orthogonal mapping. The determination of the distortion function f in this system has been the main concern of many researchers [13–15]. Unlike the TTM system proposed by Thompson *et al.* [9] which has been extended to adaptive mesh generation [1, 6, 10], no literature has reported that the RL system can be used for adaptive mesh generation. In the current study, an elliptic adaptive mesh generation system has been derived from this system according to the orthogonal condition and the equal-distribution principle.

DOI: 10.1002/fld

2.2. Orthogonality and adaptivity

In two dimensions, the Jacobin J(represents the cell area) of the transformation matrix is defined by

$$J = \begin{vmatrix} x_\xi & y_\xi \\ x_\eta & y_\eta \end{vmatrix} = x_\xi y_\eta - x_\eta y_\xi \tag{5}$$

If the orthogonal condition is satisfied, that is,

$$g_{12} = g_{21} = x_\xi x_\eta + y_\xi y_\eta = 0 \tag{6}$$

then one can obtain the Jacobin for orthogonality

$$J^* = h_\xi \cdot h_\eta \tag{7}$$

Let a ratio r be used to relate the two Jacobins defined by Equations (5) and (7), respectively,

$$J^* = r \cdot J \quad (r>0) \tag{8}$$

Equations (2), (7) and (8) lead to the following relationships:

$$f = \frac{h_\eta^2}{rJ} \tag{9a}$$

$$\frac{1}{f} = \frac{h_\xi^2}{rJ} \tag{9b}$$

Substituting Equation (9) into Equation (1) and rearranging it, one obtains:

$$-\frac{J_\xi}{J^2}\frac{h_\eta^2}{r}x_\xi - \frac{J_\eta}{J^2}\frac{h_\xi^2}{r}x_\eta + \frac{1}{J}\cdot X = 0 \tag{10a}$$

$$-\frac{J_\xi}{J^2}\frac{h_\eta^2}{r}y_\xi - \frac{J_\eta}{J^2}\frac{h_\xi^2}{r}y_\eta + \frac{1}{J}\cdot Y = 0 \tag{10b}$$

where

$$X = \frac{\partial}{\partial\xi}\left(\frac{h_\eta^2}{r}x_\xi\right) + \frac{\partial}{\partial\eta}\left(\frac{h_\xi^2}{r}x_\eta\right) \tag{11a}$$

$$Y = \frac{\partial}{\partial\xi}\left(\frac{h_\eta^2}{r}y_\xi\right) + \frac{\partial}{\partial\eta}\left(\frac{h_\xi^2}{r}y_\eta\right) \tag{11b}$$

DOI: 10.1002/fld

From Equation (10), J_ξ and J_η can be written in terms of X and Y as follows:

$$J_\xi = \frac{r}{h_\eta^2}(X \cdot y_\eta - Y \cdot x_\eta) \tag{12a}$$

$$J_\eta = \frac{r}{h_\xi^2}(Y \cdot x_\xi - X \cdot y_\xi) \tag{12b}$$

In 1982, Brackbill and Saltzman [3] developed a variational adaptive system based on the relationships among mesh orthogonality, smoothness and adaptivity. The following integral was used to measure the adaptivity.

$$I_w = \int_D (w \cdot J)\,\mathrm{d}A \tag{13}$$

According to the equal-distribution principle, when this integral is minimized, $w \cdot J$ ($w>0$) should have a uniform distribution:

$$w \cdot J = \text{const} \tag{14}$$

So that where the weighting function w is large, the cell area J should be small, and *vice versa*. Differentiation of Equation (14) with respect to ξ and η yields:

$$\frac{\partial}{\partial \xi}(w \cdot J) = 0 \quad \Rightarrow \quad J_\xi \cdot w + J \cdot w_\xi = 0 \tag{15a}$$

$$\frac{\partial}{\partial \eta}(w \cdot J) = 0 \quad \Rightarrow \quad J_\eta \cdot w + J \cdot w_\eta = 0 \tag{15b}$$

Substitution of Equation (12) into Equation (15) leads to

$$w \cdot \frac{r}{h_\eta^2}(X \cdot y_\eta - Y \cdot x_\eta) + J \cdot w_\xi = 0 \tag{16a}$$

$$w \cdot \frac{r}{h_\xi^2}(Y \cdot x_\xi - X \cdot y_\xi) + J \cdot w_\eta = 0 \tag{16b}$$

After simple algebraic manipulations of Equation (16), X and Y can be written in terms of the scale factors (h_ξ and h_η) and the weighting function w:

$$X = \frac{\partial}{\partial \xi}\left(\frac{h_\eta^2}{r} x_\xi\right) + \frac{\partial}{\partial \eta}\left(\frac{h_\xi^2}{r} x_\eta\right) = -\frac{w_\xi h_\eta^2}{w \cdot r} x_\xi - \frac{w_\eta h_\xi^2}{w \cdot r} x_\eta \tag{17a}$$

$$Y = \frac{\partial}{\partial \xi}\left(\frac{h_\eta^2}{r} y_\xi\right) + \frac{\partial}{\partial \eta}\left(\frac{h_\xi^2}{r} y_\eta\right) = -\frac{w_\xi h_\eta^2}{w \cdot r} y_\xi - \frac{w_\eta h_\xi^2}{w \cdot r} y_\eta \tag{17b}$$

DOI: 10.1002/fld

With the relationships described in Equation (9) and the chain rule of the derivatives, Equation (17) can be rewritten as the following conservative form:

$$\frac{\partial}{\partial\xi}\left(f\cdot Jw\cdot\frac{\partial x}{\partial\xi}\right)+\frac{\partial}{\partial\eta}\left(\frac{1}{f}\cdot Jw\cdot\frac{\partial x}{\partial\eta}\right)=0 \tag{18a}$$

$$\frac{\partial}{\partial\xi}\left(f\cdot Jw\cdot\frac{\partial y}{\partial\xi}\right)+\frac{\partial}{\partial\eta}\left(\frac{1}{f}\cdot Jw\cdot\frac{\partial y}{\partial\eta}\right)=0 \tag{18b}$$

Equation (18) can also be rewritten in a Poisson-like form with source terms:

$$\frac{\partial}{\partial\xi}\left(f\cdot\frac{\partial x}{\partial\xi}\right)+\frac{\partial}{\partial\eta}\left(\frac{1}{f}\cdot\frac{\partial x}{\partial\eta}\right)+P=0 \tag{19a}$$

$$\frac{\partial}{\partial\xi}\left(f\cdot\frac{\partial y}{\partial\xi}\right)+\frac{\partial}{\partial\eta}\left(\frac{1}{f}\cdot\frac{\partial y}{\partial\eta}\right)+Q=0 \tag{19b}$$

$$P=\left(\frac{J_\xi}{J}+\frac{w_\xi}{w}\right)f\cdot x_\xi+\left(\frac{J_\eta}{J}+\frac{w_\eta}{w}\right)\frac{1}{f}\cdot x_\eta \tag{19c}$$

$$Q=\left(\frac{J_\xi}{J}+\frac{w_\xi}{w}\right)f\cdot y_\xi+\left(\frac{J_\eta}{J}+\frac{w_\eta}{w}\right)\frac{1}{f}\cdot y_\eta \tag{19d}$$

where P and Q are called control functions for mesh adaptivity.

Equation (19) is an elliptic adaptive mesh generation system derived from the RL system (Equation (1)) according to the orthogonal condition (orthogonality) described by Equation (6) and the cell area equal-distribution principle (adaptivity) defined by Equation (14). The only difference between this equation and the RL system lies in the source terms P and Q. In the RL system, they are equal to zero, while in Equation (19) they are formulated based on the orthogonal condition and the equal-distribution principle. An alternative simpler way to derive this equation is to directly substitute Equation (15) into Equation (10).

Obviously, when Equation (14) is satisfied in the whole domain, Equation (18) will be reduced to the original RL system, and the control functions in Equation (19) will become zero. However, in case of uniform weighting function, a constant cell area is enforced in the whole domain, and Equation (18) or (19) does not return to the RL system. Instead, the control functions P and Q are reduced to

$$P=\frac{J_\xi}{J}f\cdot x_\xi+\frac{J_\eta}{J}\frac{1}{f}\cdot x_\eta \tag{20a}$$

$$Q=\frac{J_\xi}{J}f\cdot y_\xi+\frac{J_\eta}{J}\frac{1}{f}\cdot y_\eta \tag{20b}$$

Equation (20) proves that the proposed adaptive mesh generation system described by Equation (19) strictly satisfies the cell area equal distribution. Lee [6] pointed out that the adaptive systems developed by Winslow [10] and Anderson [1] only have approximate constraints on the cell area or arc length distribution, because the control functions they proposed are identically equal to zero with the uniform weighting function enforced.

DOI: 10.1002/fld

An immediate extension of Equation (18) is to introduce a user-specified constant parameter to control the adaptivity. That is,

$$\frac{\partial}{\partial\xi}\left[f\cdot(Jw)^{\lambda_\alpha}\cdot\frac{\partial x}{\partial\xi}\right]+\frac{\partial}{\partial\eta}\left[\frac{1}{f}\cdot(Jw)^{\lambda_\alpha}\cdot\frac{\partial x}{\partial\eta}\right]=0 \tag{21a}$$

$$\frac{\partial}{\partial\xi}\left[f\cdot(Jw)^{\lambda_\alpha}\cdot\frac{\partial y}{\partial\xi}\right]+\frac{\partial}{\partial\eta}\left[\frac{1}{f}\cdot(Jw)^{\lambda_\alpha}\cdot\frac{\partial y}{\partial\eta}\right]=0 \tag{21b}$$

where $\lambda_a(\geqslant 0)$ is used to control the intensity of the adaptivity.

And then one can obtain:

$$\frac{\partial}{\partial\xi}\left(f\cdot\frac{\partial x}{\partial\xi}\right)+\frac{\partial}{\partial\eta}\left(\frac{1}{f}\cdot\frac{\partial x}{\partial\eta}\right)+P=0 \tag{22a}$$

$$\frac{\partial}{\partial\xi}\left(f\cdot\frac{\partial y}{\partial\xi}\right)+\frac{\partial}{\partial\eta}\left(\frac{1}{f}\cdot\frac{\partial y}{\partial\eta}\right)+Q=0 \tag{22b}$$

$$P=\lambda_a\cdot\left[\left(\frac{J_\xi}{J}+\frac{w_\xi}{w}\right)f\cdot x_\xi+\left(\frac{J_\eta}{J}+\frac{w_\eta}{w}\right)\frac{1}{f}\cdot x_\eta\right] \tag{22c}$$

$$Q=\lambda_a\cdot\left[\left(\frac{J_\xi}{J}+\frac{w_\xi}{w}\right)f\cdot y_\xi+\left(\frac{J_\eta}{J}+\frac{w_\eta}{w}\right)\frac{1}{f}\cdot y_\eta\right] \tag{22d}$$

Equation (22) is more flexible than Equations (18) and (19). With the adjustable parameter λ_a, it can switch between the RL system ($\lambda_a=0$) and the adaptive RL system ($\lambda_a=1$). Note that the equal-distribution principle still holds in Equation (22). In this paper, Equation (22) will be referred as the proposed elliptic adaptive mesh generation system hereafter.

2.3. Smoothness

Derived from the RL system, Equation (22) also inherits the disadvantage of this generation system: it is lack of emphasizes on mesh smoothness. As pointed out in [13–15], the strong local orthogonal condition may cause serious mesh distortion and overlapping in geometrically complex domains, which eventually will affect mesh adaptivity. On the other hand, in regions of large gradients, the mesh may become increasingly distorted or skewed because of the equal-distribution principle (adaptivity), which may introduce new errors into the solution [16]. Therefore, smoothing is also necessary in the adaptive mesh generation.

To resolve the mesh distortion and overlapping problems in geometrically complex domains with 'weak constraint' method, Zhang *et al*. [13] used the averaged scale factors as well as the scale factors to evaluate the distortion functions. For one typical mesh node (i, j), their method

DOI: 10.1002/fld

can be described as follows:

$$f_{i,j} = \frac{(\overline{h_\eta})_j \cdot s_\eta + (h_\eta)_{i,j} \cdot (1 - s_\eta)}{(\overline{h_\xi})_i \cdot s_\xi + (h_\xi)_{i,j} \cdot (1 - s_\xi)} \tag{23a}$$

$$(\overline{h_\xi})_i = \frac{1}{N_j - 2} \sum_{j=2}^{N_j - 1} (h_\xi)_{i,j} \tag{23b}$$

$$(\overline{h_\eta})_j = \frac{1}{N_i - 2} \sum_{i=2}^{N_i - 1} (h_\eta)_{i,j} \tag{23c}$$

where $(\overline{h_\xi})_i$ and $(\overline{h_\eta})_j$ are the global-averaged scale factors at $\xi = i$ line and at $\eta = j$ line, respectively; N_i and N_j are the total number of mesh lines in ξ and η directions; and, s_η and s_ξ are two adjustable parameters within the range of [0, 1] to control the ratio between the averaged scale factors and the local scale factors and further to control the local balance of mesh orthogonality and smoothness.

The two parameters s_η and s_ξ can be either user specified or automatically adjusted according to the local smoothness condition

$$(s_\xi)_{i,j} = \frac{|(h_\xi)_{i,j} - (\overline{h_\xi})_i|}{(h_\xi)_{i,j} + (\overline{h_\xi})_i} \tag{24a}$$

$$(s_\eta)_{i,j} = \frac{|\,(h_\eta)_{i,j} - (\overline{h_\eta})_j\,|}{(h_\eta)_{i,j} + (\overline{h_\eta})_j} \tag{24b}$$

In this study, this method is adopted to reduce the mesh distortion and improve the mesh smoothness. With Equation (23), mesh smoothness is controlled by the empirical parameters s_η and s_ξ which in turn influences mesh orthogonality and adaptivity. In general, the larger they are, the produced mesh will be smoother but less orthogonal and less adaptive (less equally distributed weighting function) and *vice versa*. Obviously, when s is equal to zero, Equation (23) will turn to Equation (2)—the original definition of the distortion function.

2.4. Mesh quality

According to the truncation error analysis [17], the errors on the solutions brought by a computational mesh lie in two aspects: non-orthogonality and non-uniformity (non-smoothness). Thus, it is well accepted that mesh quality is measured by two standard academic criterions: mesh orthogonality and smoothness. As for mesh adaptivity, it becomes more and more important in practical problems due to its capability of improving the accuracy of solutions. Unfortunately, in practice it is very difficult and nearly impossible to fully maintain these three criterions simultaneously in one mesh. Even producing an optimal combination of them still remains a challenge. In the previous studies on adaptive mesh generation, usually mesh adaptivity was the most concerned and the other aspects of mesh quality, such as orthogonality and smoothness, were ignored. For example, in the elliptic adaptive systems developed from the TTM system [1, 6, 10], only the mesh adaptivity was considered; and, the variational system proposed by Brackbill and Saltzman [3] considers only a user-specified combination of mesh orthogonality, smoothness and adaptivity which influence and compromise each other. Compared with other methods, the proposed adaptive mesh generation

DOI: 10.1002/fld

system defined by Equation (22) considers both orthogonality and adaptivity simultaneously since the orthogonal condition and the equal-distribution principle are enforced during the derivation, which is one important and unique feature. This feature is attractive and crucial for the application of the adaptive mesh generation, since the negative effects of mesh adaptivity on the overall mesh quality is reduced greatly. However, as stated previously, a drawback lies in the possible mesh distortion caused by the local orthogonal condition, which would influence the overall mesh quality.

2.5. Weighting function

An adaptive algorithm consists of two main parts: the adaptive mesh generation system and the weighting function. The success of the application of an adaptive algorithm to the real problems depends largely on the weighing function which guides the relocation of mesh nodes [16]. Usually, the weighting function is selected to represent the characteristic of the solution. In [16], some typical weighing functions based on the error estimators were reviewed. In [17], Thompson *et al.* lists some weighting functions constructed according to the solution gradient. However, the construction of the weighting function is beyond the focus of the current study, so the weighting functions used in the examples and application of this paper will be directly given without explanations.

2.6. Discretization

The discretization of Equation (22) at one typical mesh node (i, j) using the central difference scheme is identical to that of Equation (1). One can easily obtain:

$$F_{i,j}x_{i,j} = f_{i+1/2,j}x_{i+1,j} + f_{i-1/2,j}x_{i-1,j} + \frac{1}{f_{i,j+1/2}}x_{i,j+1} + \frac{1}{f_{i,j-1/2}}x_{i,j-1} + P_{i,j} \tag{25a}$$

$$F_{i,j}y_{i,j} = f_{i+1/2,j}y_{i+1,j} + f_{i-1/2,j}y_{i-1,j} + \frac{1}{f_{i,j+1/2}}y_{i,j+1} + \frac{1}{f_{i,j-1/2}}y_{i,j-1} + Q_{i,j} \tag{25b}$$

where

$$F_{i,j} = f_{i+1/2,j} + f_{i-1/2,j} + \frac{1}{f_{i,j+1/2}} + \frac{1}{f_{i,j-1/2}}$$

Note that the distortion functions in the first four terms of the right-hand side of Equation (25) are evaluated using Equation (23), while in the control functions P and Q the distortion function remains its original definition.

3. SOLUTION PROCESS

The highly non-linear Poisson equation system defined by Equation (19) is solved using an iterative algorithm, which is simply listed as follows:

1. Define the boundaries of the domain and use an algebraic method to generate an initial mesh.
2. Calculate the weighting functions w.
3. Specify the adaptive parameter λ_a.

DOI: 10.1002/fld

4. Calculate the distortion function f from Equation (23).
5. Calculate the control functions P and Q using the most recent solution from Equations (22c) and (22d).
6. Solve Equation (25) with fixed f obtained from step 3.
7. Update the mesh and check if the convergence condition is satisfied. If not, repeat steps from 2 through 6.

Two convergence criterions are used and the satisfaction of either one will stop the computation. The first one is the maximum difference between the grid coordinates in consecutive steps and the second one is the maximum relative difference of the distortion function f between consecutive iterations. They are defined as follows:

$$\max\left(\sqrt{(x_{i,j}^n - x_{i,j}^{n-1})^2 + (y_{i,j}^n - y_{i,j}^{n-1})^2}\right) < 10^{-6} \tag{26}$$

$$\max\left(\frac{f^n - f^{n-1}}{f^n}\right) < 10^{-6} \tag{27}$$

where n is the iteration number.

4. BOUNDARY CONDITIONS

Two types of boundary conditions are available: the Dirichlet boundary condition with the fixed specified nodal distribution along the boundaries, and the Dirichlet–Neumann boundary condition (also called sliding boundary condition) which allows the mesh nodes slide along the boundaries (Dirichlet) to satisfy the Neumann condition.

In the current study, both boundary conditions will be used to test the proposed method.

5. EXAMPLES

A typical location-based adaptive method, Lee's method [6], is selected to compare with the current method, since this method is a good representative of the group of adaptive mesh generation systems derived from TTM system [9]. The adaptive generation system proposed by Lee [6] can be described as follows:

$$g_{22}\frac{\partial^2 x}{\partial \xi^2} - 2g_{12}\frac{\partial^2 x}{\partial \xi \partial \eta} + g_{11}\frac{\partial^2 x}{\partial \eta^2} + g\left(P_x\frac{\partial x}{\partial \xi} + Q_x\frac{\partial x}{\partial \eta}\right) = 0 \tag{28a}$$

$$g_{22}\frac{\partial^2 y}{\partial \xi^2} - 2g_{12}\frac{\partial^2 y}{\partial \xi \partial \eta} + g_{11}\frac{\partial^2 y}{\partial \eta^2} + g\left(P_y\frac{\partial y}{\partial \xi} + Q_y\frac{\partial y}{\partial \eta}\right) = 0 \tag{28b}$$

where P and Q are control functions in the form of

$$(P_x, P_y) = \frac{1}{g}\left[g_{22}\frac{w_\xi}{w} - g_{12}\frac{w_\eta}{w} - (x, y)_\xi (x, y)_{\eta\eta} + (x, y)_\eta (x, y)_{\xi\eta}\right] \tag{29a}$$

$$(Q_x, Q_y) = \frac{1}{g}\left[g_{11}\frac{w_\eta}{w} - g_{12}\frac{w_\xi}{w} - (x, y)_\eta (x, y)_{\xi\xi} + (x, y)_\xi (x, y)_{\xi\eta}\right] \tag{29b}$$

DOI: 10.1002/fld

where the subscripts 'ξ' and '$\xi\xi$' denote the first and second derivatives with respect to ξ, respectively, and so on.

Three benchmarking examples used by Cao *et al.* [4] in a rectangular domain with both width and height equal to 1 are selected to illustrate and compare the current method with Lee's method. The weighting functions for these three examples are defined as follows and the distribution of these three weighting functions is shown in Figure 1.

- *Example A* (*time independent*):

$$w(x, y) = 1 + 10 \exp\{[-50(y - 0.5 - 0.25 \sin(2\pi x))]^2\} \tag{30}$$

- *Example B* (*time independent*):

$$w(x, y) = 1 + 10 \exp[-50 \,|\, (x - 0.5)^2 + (y - 0.5)^2 - (\tfrac{1}{4})^2 \,|] \tag{31}$$

- *Example C* (*time dependent*):

$$\begin{aligned} w(x, y, t) = 1 + 10 \exp\{[-50 \,|\, (x - 0.5 - 0.25 \cos(2\pi t))^2 \\ +(y - 0.5 - 0.25 \sin(2\pi t))^2 - (\tfrac{1}{10})^2 \,|]\} \end{aligned} \tag{32}$$

Since the goal of the adaptive mesh generation is to produce non-uniform meshes with controlled density distribution, in this study the mesh quality is characterized only by mesh orthogonality and adaptivity. The mesh orthogonality is evaluated quantitatively by maximum deviation orthogonality (MDO) and averaged deviation from orthogonality (ADO), which are defined as follows:

$$\mathrm{MDO} = \max(\theta_{i,j}) \tag{33a}$$

$$\mathrm{ADO} = \frac{1}{(N_i - 2)} \frac{1}{(N_j - 2)} \sum_{2}^{N_i - 1} \sum_{2}^{N_j - 1} \max(\theta_{i,j}) \tag{33b}$$

where N_i and N_j are the maximum number of mesh lines in ξ and η directions respectively; and θ is defined as

$$\theta_{i,j} = \left| \arccos\left(\frac{g_{12}}{h_\xi h_\eta} \right)_{i,j} - 90 \right| \tag{34}$$

The normalized cell-distributed weighting function EP is used to quantitatively measure the mesh adaptivity. The closer to 1 it is, the better adaptivity the mesh will have.

$$\mathrm{EP} = \mathrm{ED}/\overline{\mathrm{ED}} \tag{35a}$$

$$\mathrm{ED} = J \cdot w \tag{35b}$$

$$\overline{\mathrm{ED}} = \frac{1}{(N_i - 2)} \frac{1}{(N_j - 2)} \sum_{2}^{N_i - 1} \sum_{2}^{N_j - 1} (\mathrm{ED}) \tag{35c}$$

where EP can measure how close to the equal distribution the weighting function is and $\overline{\mathrm{ED}}$ is the averaged cell-distributed weighting function.

DOI: 10.1002/fld

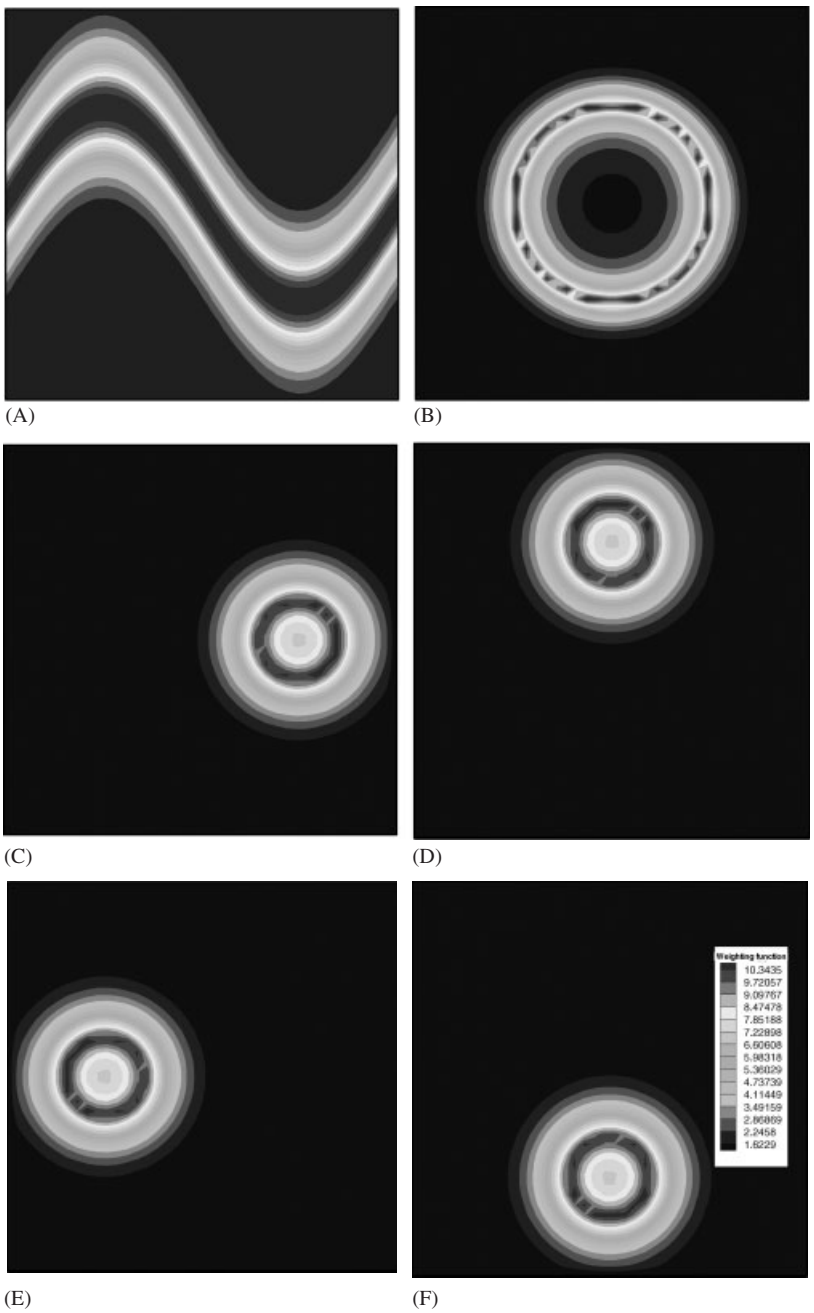

Figure 1. Distribution of weighting functions: (A) example A; (B) example B; (C) example C ($t = 0$); (D) example C ($t = 0.25$); (E) example C ($t = 0.5$); and (F) example C ($t = 0.75$).

DOI: 10.1002/fld

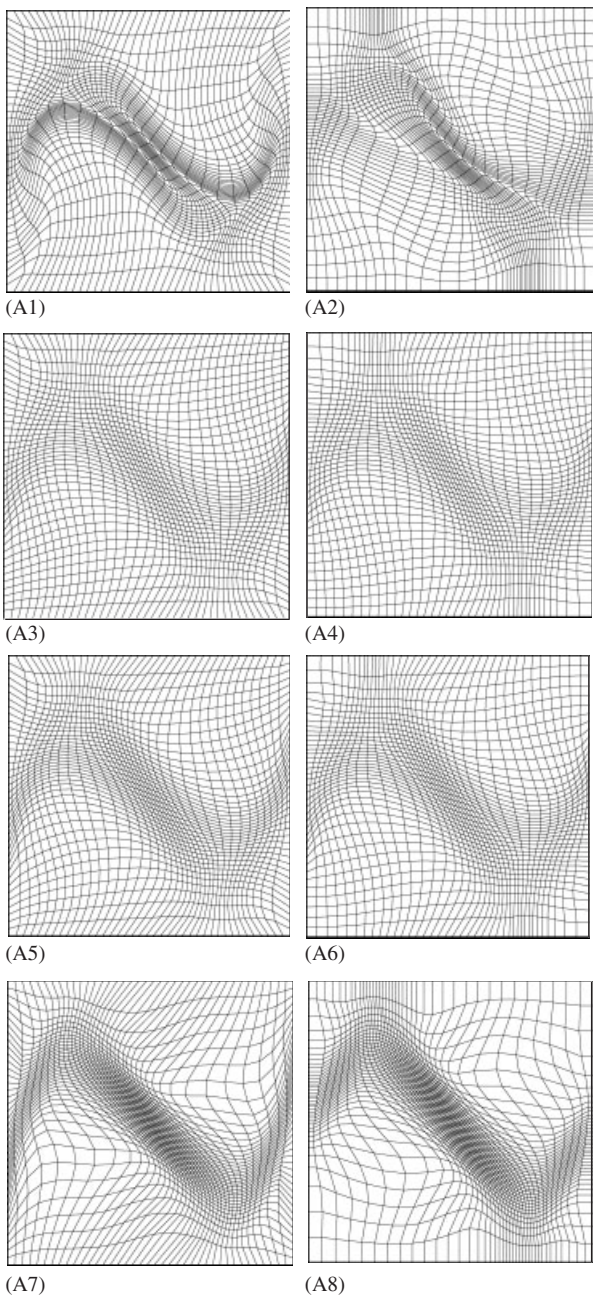

Figure 2. Adaptive meshes for example A: (A1) current method (Dirichlet B.C.) with $\lambda_a = 1$ and $s_\xi = s_\eta = 0$; (A2) current method (sliding B.C.) with $\lambda_a = 1$ and $s_\xi = s_\eta = 0$; (A3) current method (Dirichlet B.C.) with $\lambda_a = 1.0$; (A4) current method (sliding B.C.) with $\lambda_a = 1.0$; (A5) current method (Dirichlet B.C.) with $\lambda_a = 2.0$; (A6) current method (sliding B.C.) with $\lambda_a = 2.0$;(A7) Lee's method (Dirichlet B.C.); and (A8) Lee's method (sliding B.C.).

DOI: 10.1002/fld

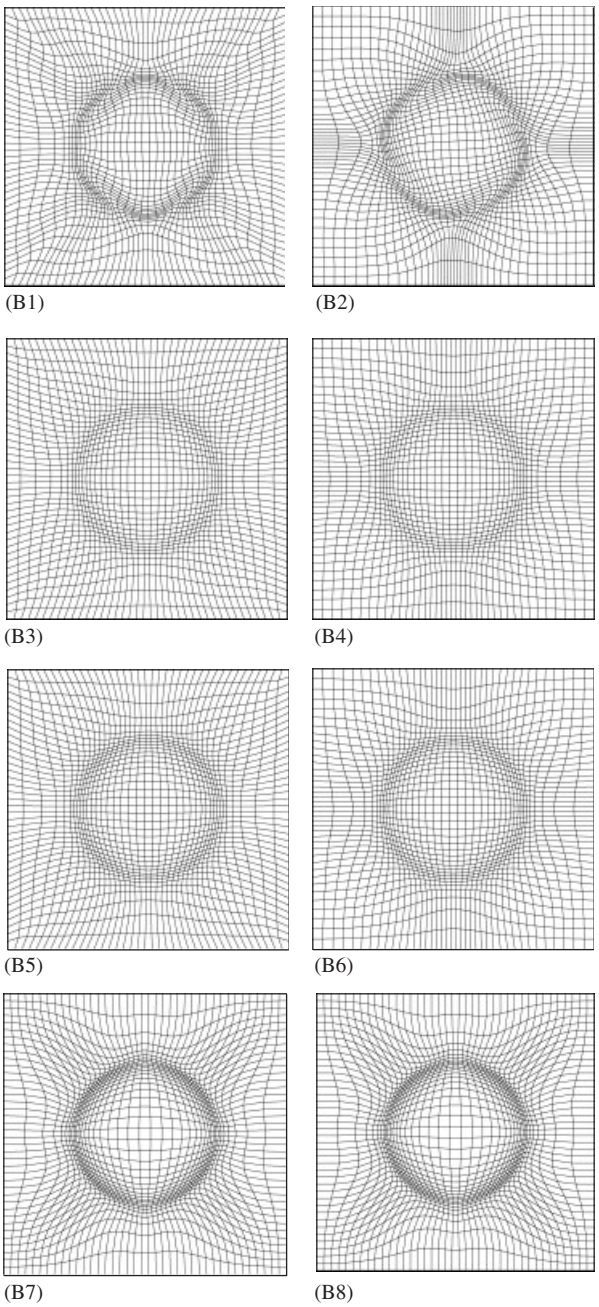

Figure 3. Adaptive meshes for example B: (B1) current method (Dirichlet B.C.) with $\lambda_a = 1$ and $s_\xi = s_\eta = 0$; (B2) current method (sliding B.C.) with $\lambda_a = 1$ and $s_\xi = s_\eta = 0$; (B3) current method (Dirichlet B.C.) with $\lambda_a = 1.0$; (B4) current method (sliding B.C.) with $\lambda_a = 1.0$; (B5) current method (Dirichlet B.C.) with $\lambda_a = 2.0$; (B6) current method (sliding B.C.) with $\lambda_a = 2.0$; (B7) Lee's method (Dirichlet B.C.); and (B8) Lee's method (sliding B.C.).

DOI: 10.1002/fld

Table I. Mesh evaluation for example A.

Example	Case	Size	EP_{min}	EP_{max}	ADO	MDO	λ_a	s_ξ, s_η
A	A1	40×40	0.418	1.851	12.34	62.9	1.0	0
	A2	40×40	0.664	1.546	7.9	52.3	1.0	0
	A3	40×40	0.363	1.752	17.66	44.36	1.0	Equation (24)
	A4	40×40	0.421	1.642	15.06	41.8	1.0	Equation (24)
	A5	40×40	0.45	1.561	23.7	55.68	2.0	Equation (24)
	A6	40×40	0.511	1.432	21.0	53.0	2.0	Equation (24)
	A7	40×40	0.420	2.086	42.3	77.8	—	—
	A8	40×40	0.534	2.122	41.1	79.0	—	—

Table II. Mesh evaluation for example B.

Example	Case	Size	EP_{min}	EP_{max}	ADO	MDO	λ_a	s_ξ, s_η
B	B1	40×40	0.595	1.773	11.59	32.62	1.0	0
	B2	40×40	0.678	1.668	7.99	25.72	1.0	0
	B3	40×40	0.599	1.743	13.37	29.7	1.0	Equation (24)
	B4	40×40	0.675	1.721	10.32	28.63	1.0	Equation (24)
	B5	40×40	0.695	1.449	16.79	38.89	2.0	Equation (24)
	B6	40×40	0.758	1.428	13.79	36.77	2.0	Equation (24)
	B7	40×40	0.451	1.584	28.15	60.76	—	—
	B8	40×40	0.469	1.583	27.95	60.73	—	—
	B9	40×40	0.596	1.781	11.82	32.12	1.0	0
	B10	40×40	0.662	1.734	8.02	25.54	1.0	0

For all cases except B7 and B8, a uniform initial meshes (40×40) with uniform nodal distribution along the four boundaries is generated by the algebraic method, namely, top boundary, bottom boundary, left boundary and right boundary.

5.1. Time-independent examples

The adaptive meshes for examples A and B are illustrated in Figures 2 and 3, respectively. And, the quality of the final meshes with different configurations is summarized in Tables I and II.

In example A, both methods successfully produced high mesh density in regions with high weighting values. Compared to Lee's method (cases A7 and A8), the current method (cases A1–A6) has better performances in both mesh orthogonality and adaptivity. Although there is little difference in mesh adaptivity between two methods, the current method produced much more orthogonal meshes. For current method, skewed meshes, which cause discontinuous transition of the mesh density distribution, exist in cases A1 and A2 due to the local strong orthogonal condition [13–15]. As for cases A3–A6, with consideration of mesh smoothness ($s_\xi, s_\eta > 0$), both mesh smoothness and the transition have been significantly improved at little cost of mesh orthogonality. In cases A5–A6, the mesh adaptivity is emphasized ($\lambda_a = 2.0$), and the mesh adaptivity is further improved with degenerated mesh orthogonality. Among all cases, case A4 with consideration of mesh smoothness and the application of the sliding boundary condition has the best overall quality.

DOI: 10.1002/fld

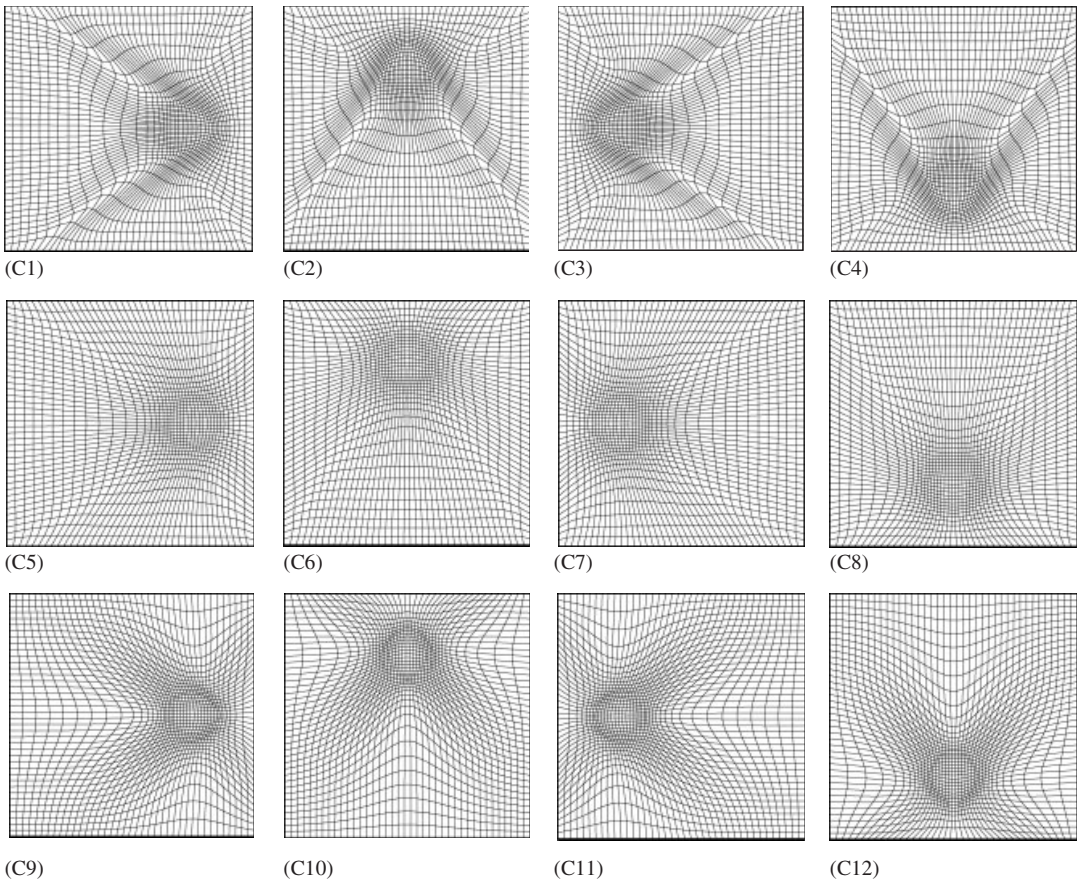

Figure 4. Adaptive meshes for example C using Dirichlet boundary condition. For C1–C4, $\lambda_a = 1$ and $s_\xi = s_\eta = 0$; and, for C5–C8, $\lambda_a = 2$ and s_ξ, $s_\eta > 0$: (C1) current method ($t = 0$); (C2) current method ($t = 0.25$); (C3) current method ($t = 0.5$); (C4) current method ($t = 0.75$); (C5) current method ($t = 0$); (C6) current method ($t = 0.25$); (C7) current method ($t = 0.5$); (C8) current method ($t = 0.75$); (C9) Lee's method ($t = 0$); (C10) Lee's method ($t = 0.25$); (C11) Lee's method ($t = 0.5$); and (C12) Lee's method ($t = 0.75$).

In example B, similarly, both methods have close performances on mesh adaptivity, and the current method (cases B1–B6) is much better in mesh orthogonality than Lee's method (cases B7 and B8). For current method, compared to cases B1 and B2, the overall mesh quality in both orthogonality and adaptivity have been improved in cases B3–B6 with considering mesh smoothness. With larger λ_a, cases B5 and B6 produced more adaptive meshes than cases B3–B4.

In example B, the distribution of the weighting function in the whole domain is symmetric. Compared to example A with asymmetric distribution of weighting function, only slight transition problem exists in cases B1 and B2.

In both examples and for both methods, the sliding boundary condition produced meshes with better quality than the Dirichlet boundary condition.

DOI: 10.1002/fld

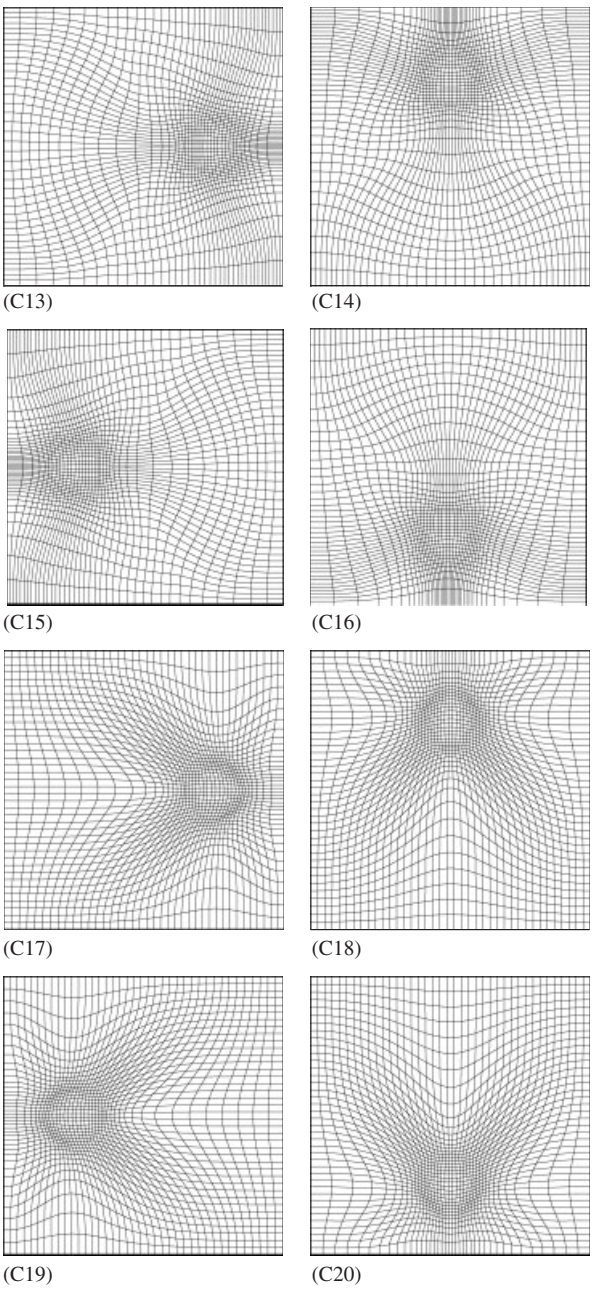

Figure 5. Adaptive meshes for example C using sliding boundary condition. For C13–C20, $\lambda_a = 1$ and $s_\xi = s_\eta = 0$: (C13) current method ($t = 0$); (C14) current method ($t = 0.25$); (C15) current method ($t = 0.5$); (C16) current method ($t = 0.75$); (C17) Lee's method ($t = 0$); (C18) Lee's method ($t = 0.25$); (C19) Lee's method ($t = 0.5$); and (C20) Lee's method ($t = 0.75$).

DOI: 10.1002/fld

Table III. Mesh evaluation for example C.

Example	Case	Size	EP_{min}	EP_{max}	ADO	MDO	λ_a	s_ξ, s_η
C	C1–C4	40×40	0.649	1.449	7.0	41.88	1.0	0
	C5–C8	40×40	0.713	1.670	13.82	39.14	2.0	Equation (24)
	C9–C12	40×40	0.539	1.699	24.69	63.19	—	—
	C13–C16	40×40	0.821	1.201	3.12	12.91	1.0	0
	C17–C20	40×40	0.567	1.482	22.48	63.0	—	—

5.2. Time-dependent example

Example C is time dependent, and the solution process described previously is carried out along a time axis. In the computation, for both methods, the time step is set to 0.01 and the total time is 1. Figures 4 and 5 display the adaptive meshes for both methods at four time instances ($t = 0, 0.25, 0.5$ and 0.75) using different boundary conditions, and Table III lists the evaluation report of the final meshes.

For the Dirichlet boundary condition, the EP value varies from 0.651 to 1.848 during the computation for the current method, and from 0.530 to 1.700 for Lee's method; while for the sliding boundary condition, the EP value lies in a range of 0.749–1.448 for current method and 0.540 to 1.512 for Lee's method.

For both boundary conditions, not surprisingly, cases (C1–C8, and C13–C16) using the current method which considers mesh orthogonality and adaptivity simultaneously performed much better in both mesh orthogonality and adaptivity than their counterparts (C9–C12, and C17–C20) using Lee's method, although slightly skewed meshes were observed in cases C1–C4 with the Dirichlet boundary conditions. Compared to cases C1–C4, cases C5–C8 considered mesh smoothness and had more emphasis on mesh adaptivity. The best overall quality meshes were obtained by the current method with the sliding boundary conditions.

In this example, the distribution of weighting function is globally asymmetric but locally symmetric, and little discontinuous transition of mesh density distribution occurred in cases C1–C4 with the Dirichlet boundary conditions.

5.3. Sensitivity analysis

Example B is also used to study the effects of parameter λ_a on mesh orthogonality and adaptivity. Different values of λ_a ranging from 1 to 2.2 are used to generate the adaptive meshes using the current method.

Figure 7 illustrates the relationships between λ_a and the indicators of mesh quality (EP_{min}, EP_{max}, ADO and MDO) with the Dirichlet boundary condition. Basically, the parameter λ_a has positive influences on mesh adaptivity. As shown in Figure 7, with λ_a increasing, EP_{min} increases and EP_{max} decreases (more adaptivity). As for mesh orthogonality, with λ_a increasing, both ADO and MDO increases (less orthogonality).

According to the numerical tests, larger value of the adaptivity parameter λ_a may cause stability problems. Therefore, it must be bounded. The range from 1.0 to 2.0 is recommended for most cases. For complex domains, the range needs to be further narrowed.

To test if the current method is sensitive to the initial condition, two adaptive meshes for example B were generated using the final mesh of case A1 as the initial condition. The resulting meshes

DOI: 10.1002/fld

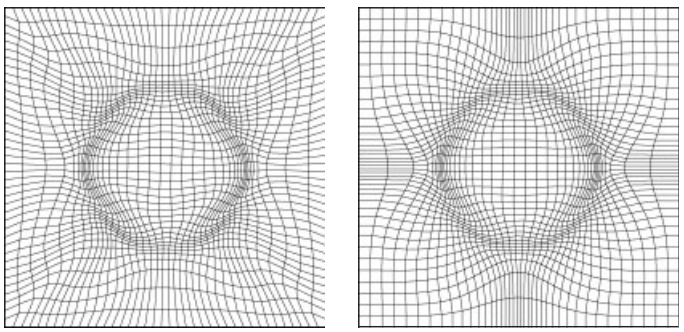

Figure 6. Adaptive meshes for example B using Case A1 as initial mesh: (B9) current method (Dirichlet B.C.) with $\lambda_a = 0$ and (B10) current method (sliding B.C.) with $\lambda_a = 0$.

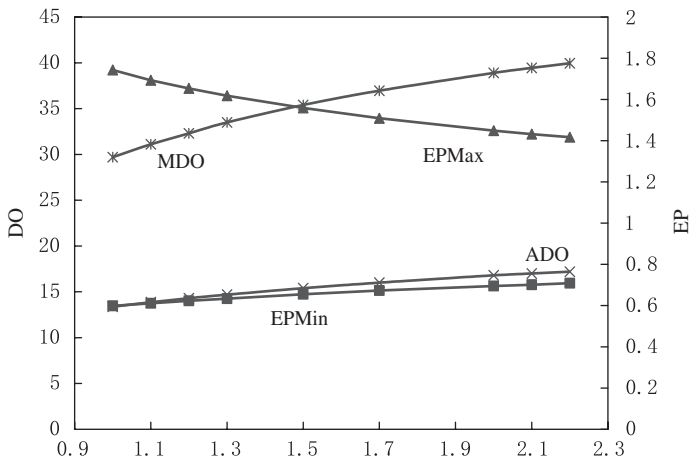

Figure 7. Effects of λ_a on mesh orthogonality and adaptivity.

(cases B9 and B10) are shown in Figures 6 and their evaluations can be found in Table II. Both cases have very close performances to their counterparts (cases B1 and B2), which indicates that the current method is stable and not sensitive to the initial conditions.

6. APPLICATION

To further challenge the proposed method, a natural curved channel (domain D) is selected and its layout is illustrated in Figure 8. As shown in Figure 8 (A), the main channel is narrow and deep compared to the floodplains most of which will be dry in the dry season. With much less concerns, it is desirable to put less meshes on the floodplains. Thus, a depth adaptive mesh is obviously more suitable than an orthogonal non-adaptive mesh for this domain. The weighting function is

DOI: 10.1002/fld

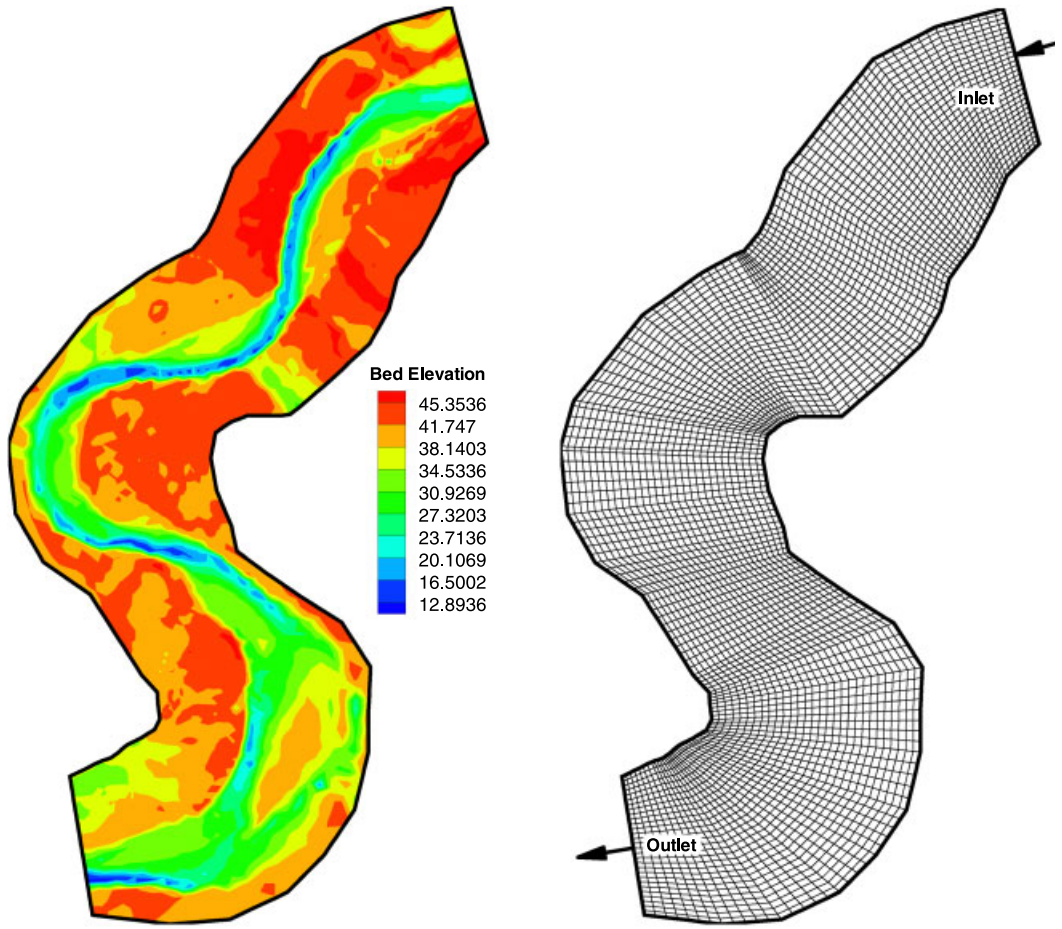

Figure 8. Domain D: (A) topography and (B) algebraic mesh.

described as follows:

$$w_{i,j} = 1.0 + (Z_{\max} - Z_{i,j}) + \sqrt{(Z_\xi^2 + Z_\eta^2)_{i,j}} \tag{36}$$

where Z and $Z_{\max}$ are nodal bed elevation and the maximum bed elevation.

Figure 9 displays the non-adaptive mesh (case D1) generated by the original RL system and the adaptive mesh (case D2) produced by current method. Table IV summarizes their evaluation. Both meshes have close evaluations on mesh orthogonality, although case D1 is slightly better. The EP value of case D2 is in the reasonable range, and more meshes are produced in the main channel.

A steady flow simulation is performed on both meshes. The water surface elevation of 34.3 m is imposed at the downstream end, while a discharge of 350.0 m^3/s is imposed on the upstream end of the channel. Figure 10 shows the velocity fields for both meshes. As can be seen, the simulation results based on the adaptive mesh is much better than the non-adaptive mesh, although

DOI: 10.1002/fld

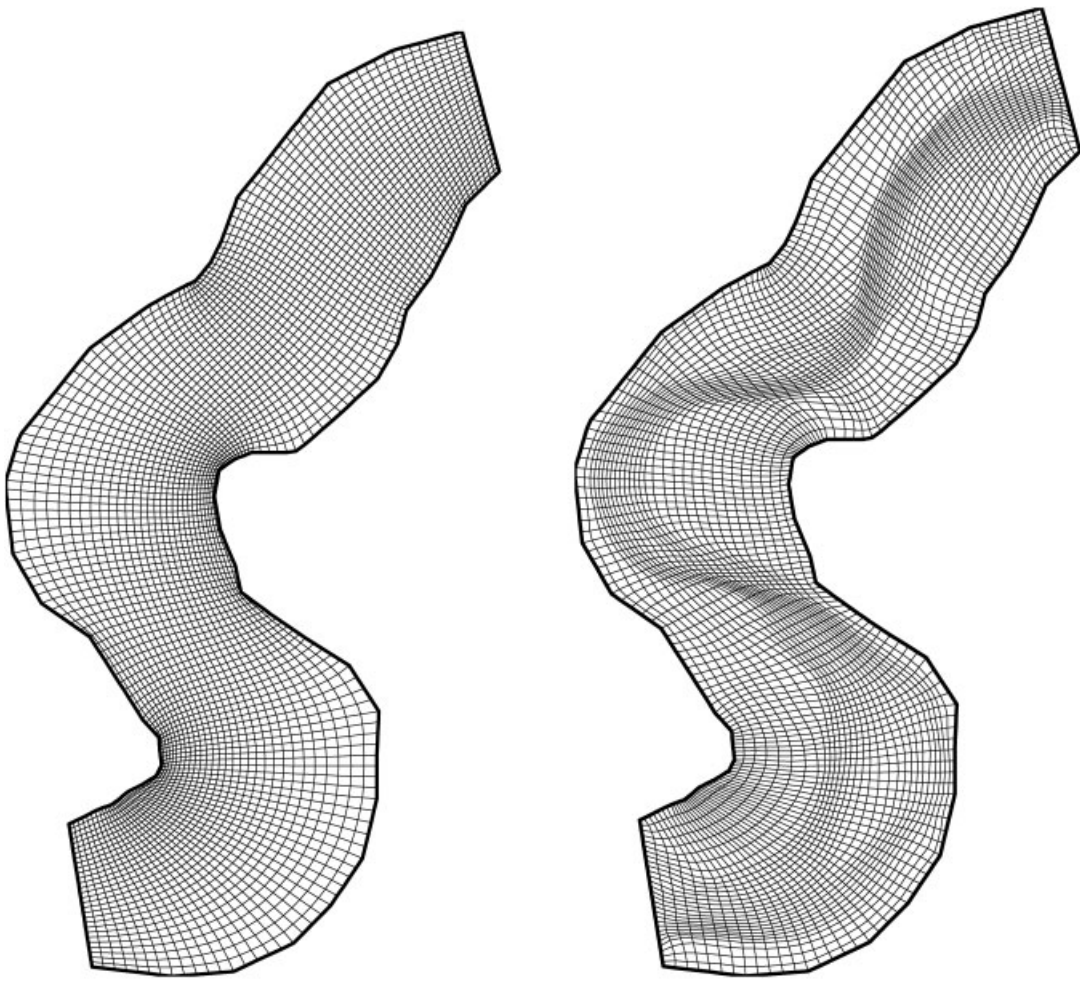

Figure 9. Meshes for domain D: (D1) non-adaptive mesh and (D2) adaptive mesh with $\lambda_a = 1.0$.

Table IV. Mesh evaluation for domain D.

Domain	Case	Size	EP_{min}	EP_{max}	ADO	MDO	λ_a	s_ξ, s_η
D	D1	30×150	0.058	6.714	7.18	43.67	—	—
	D2	30×150	0.374	1.996	13.5	50.71	1.0	Equation (24)

the latter is better in both orthogonality and smoothness. The reason lies in the fact that, in the non-adaptive mesh, few mesh lines are put in the main channel (wet part), which influences the accuracy significantly. In case D1 (non-adaptive mesh), only 20.8% of mesh nodes are wet, while in case D2 (adaptive mesh), 41.4% of mesh nodes are wet.

DOI: 10.1002/fld

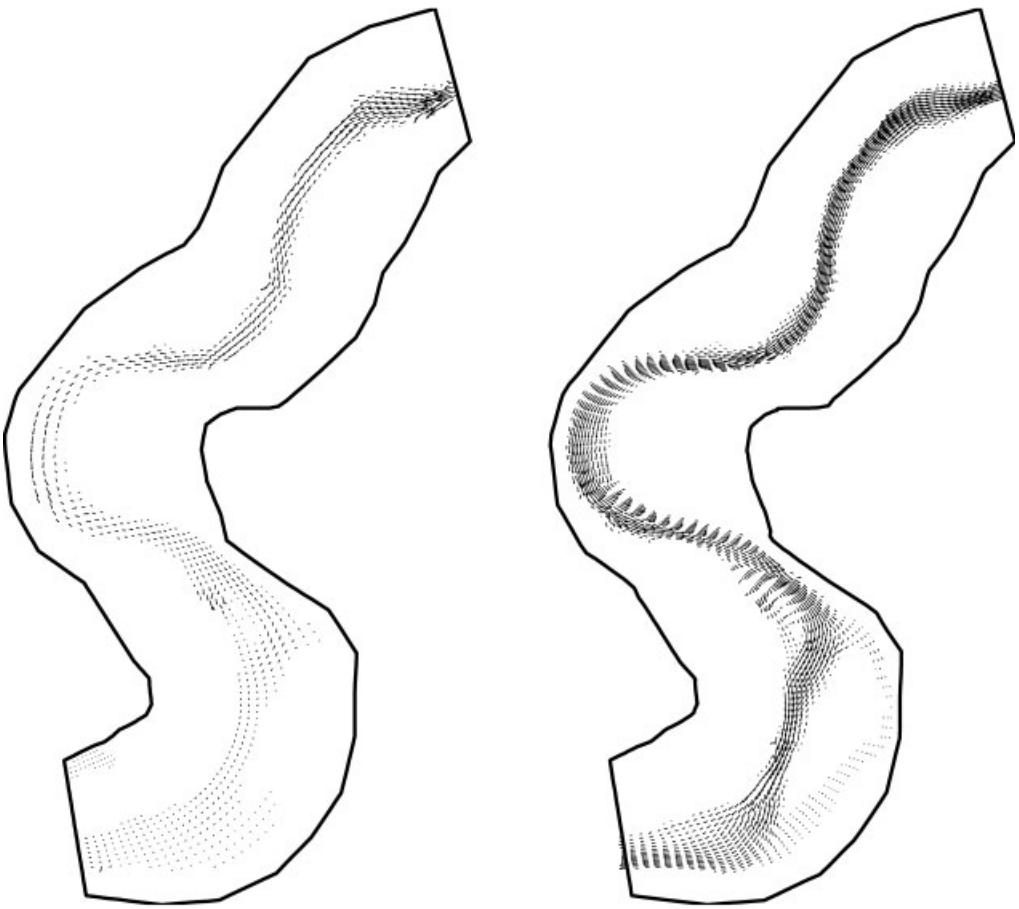

Figure 10. Velocity fields in domain D: (D1) non-adaptive mesh and (D2) adaptive mesh.

7. CONCLUSIONS

Mesh quality has significant influence on the solutions. In addition to mesh orthogonality and smoothness, the adaptive mesh density control is required in many cases of CFD analysis. In this paper, a 2D elliptic adaptive mesh generation system has been developed from a well-known orthogonal mapping system—RL system proposed by Ryskin and Leal [12].

Without any assumptions in the derivation, this adaptive generation system satisfies the orthogonal condition and the equal-distribution principle strictly. A unique feature of this system differing from other adaptive systems is that it is capable of maintaining mesh orthogonality and adaptivity simultaneously in a mesh. With introducing the averaged scale factors to evaluate the distortion function [13], it can take into account of mesh smoothness as well.

Several academic examples are selected to test and illustrate the proposed system. For all cases, compared to other method, this system has better overall performances in mesh orthogonality,

DOI: 10.1002/fld

adaptivity and smoothness, although skewed meshes exist in some cases with Dirichlet boundary conditions if no mesh smoothness is considered ($s_\xi = s_\eta = 0$). The discontinuous transition of the mesh density distribution was found in domains with locally asymmetric distribution of weighting function, which is caused by the local strong orthogonal condition. With considering mesh smoothness, both the transition and mesh smoothness were improved greatly at little sacrifice of orthogonality and smoothness. Two types of boundary conditions, namely, the Dirichlet boundary condition and the sliding boundary condition, were also compared. It is concluded that the sliding boundary condition is more suitable for adaptive mesh generation.

According to the sensitivity analysis, in this system, the adaptivity parameter λ_a which controls the intensity of mesh adaptivity generally has negative effects on mesh orthogonality. That is, the larger λ_a is (more adaptivity), the less orthogonal the resulting mesh will be. It is also found that the proposed system is stable and not sensitive to the initial conditions.

The proposed system is applied to the depth adaptive mesh generation in a natural channel. Compared with the non-adaptive mesh which satisfies mesh orthogonality and smoothness, the adaptive mesh produced much better simulation results.

ACKNOWLEDGEMENTS

This work is a result of research sponsored by the USDA Agriculture Research Service under Specific Research Agreement No. 58-6408-2-0062 (monitored by the USDA-ARS National Sedimentation Laboratory) and The University of Mississippi.

REFERENCES

1. Anderson DA. Adaptive grid scheme controlling cell area volume. *AIAA Paper 87-0202*, *AIAA 25th Aerospace Sciences Meeting*, Reno, NY, January 1987.
2. Arina R. Orthogonal grids with adaptive control. In *First International Conference on Numerical Grid Generation in CFD*, Hauser J, Taylor C (eds). Pineridge: Swansea, 1986.
3. Brackbill JU, Saltzman JS. Adaptive zoning for singular problems in two-dimensions. *Journal of Computational Physics* 1982; **46**:342–368.
4. Cao WM, Huang WZ, Russell RD. Approaches for generating moving adaptive meshes: location versus velocity. *Applied Numerical Mathematics* 2003; **47**:121–138.
5. Knupp PM. Jacobian-weighted elliptic grid generation. *SIAM Journal on Scientific Computing* 1996; **17**: 1475–1490.
6. Lee K. Elliptic adaptive grid generation and area equal-distribution. *International Journal for Numerical Methods in Fluids* 1999; **30**:481–491.
7. Liao GJ, Anderson D. A new approach to grid generation. *Applicable Analysis* 1992; **44**:285–298.
8. Sun WW. Two-dimensional mesh redistribution and solution of singular boundary value problems. *Communications in Numerical Mechanical Engineering* 1998; **14**:797–808.
9. Thompson JF, Thames FC, Mastin CW. TOMCAT—a code for numerical generation of boundary-fitted curvilinear coordinate system on fields containing any number of arbitrary two-dimensional bodies. *Journal of Computational Physics* 1977; **24**:274–302.
10. Winslow A. Adaptive mesh zoning by the equipotential method. *Lawrence Livemore National Laboratory Report UCID-19062*, University of California, 1981.
11. Chen WL, Lien FS, Leschziner MA. Local mesh refinement within a multi-block structured-grid scheme for general flows. *Computer Methods in Applied Mechanics and Engineering* 1997; **144**:327–369.
12. Ryskin G, Leal LG. Orthogonal mapping. *Journal of Computational Physics* 1983; **50**:71–100.
13. Zhang YX, Jia YF, Wang SSY. 2D nearly orthogonal mesh generation with controls on distortion functions. *Journal of Computational Physics* 2006; **218**(2):549–571.
14. Zhang YX, Jia YF, Wang SSY. 2D nearly orthogonal mesh generation. *International Journal for Numerical Methods in Fluids* 2004; **46**:685–707.

DOI: 10.1002/fld

15. Zhang YX, Jia YF, Wang SSY. Structured mesh generation with smoothness controls. *International Journal for Numerical Methods in Fluids* 2006; **51**:1255–1276.
16. McRae DS. Adaptive mesh algorithm—a review of progress and future research needs. *AIAA Paper 2001-2551* 2001.
17. Thompson JF, Warsi ZUA, Mastin CW. *Numerical Grid Generation*: *Foundation and Application*. North-Holland: New York, 1985.

DOI: 10.1002/fld